A Conformational Change of the Photoactive Bacteriopheophytin in Reaction Centers from *Rhodobacter sphaeroides*†

Frank Müh,‡ JoAnn C. Williams,§ James P. Allen,§ and Wolfgang Lubitz*,‡

Max-Volmer-Institut für Biophysikalische Chemie und Biochemie, Technische Universität Berlin, Strasse des 17, Juni 135, D-10623 Berlin, Germany, and Department of Chemistry and Biochemistry and Center for the Study of Early Events in Photosynthesis, Arizona State University, Tempe, Arizona 85287-1604

Received April 9, 1998; Revised Manuscript Received July 16, 1998

ABSTRACT: It is demonstrated by ENDOR and Special TRIPLE spectroscopy that two distinct radical anion states of the intermediate electron acceptor (I), a bacteriopheophytin, can be freeze-trapped in isolated photosynthetic reaction centers of *Rhodobacter sphaeroides*. The formation of these states depends on the illumination time prior to freezing and the temperature. The first state, $I_1^{\bullet-}$, is metastable and relaxes *irreversibly* at $T \approx 160$ K to the second state, $I_2^{\bullet-}$. Experiments on quinone depleted as well as mutant reaction centers help to exclude the possibility that other cofactors besides the bacteriopheophytin in the A-branch, Φ_A, are reduced during the trapping procedure. In particular, two mutants are investigated, in which the hydrogen bonds to Φ_A that exist in the wild type are removed. These mutants are EL(L104), in which Glu at position L104 near the 13^1-keto group of Φ_A is replaced by Leu, and WF(L100), in which Trp at position L100 near the 13^2-methyl ester of Φ_A is replaced by Phe. Both mutations have characteristic effects on both $I^{\bullet-}$ states. In addition, the replacement of Thr at position M133 near the 13^1-keto group of the inactive bacteriopheophytin and of Gly at position M203 near the 13^1-keto group of the accessory bacteriochlorophyll in the A-branch by Asp causes no changes of the electronic structure of $I^{\bullet-}$. The two $I^{\bullet-}$ states are interpreted in terms of a reorientation of the 3-acetyl group of Φ_A after reduction. Possible implications for the initial charge separation process are discussed.

In the photosynthetic reaction center (RC)[1] of purple bacteria, light-induced electron transfer (ET) leads to a stable charge separation with high quantum yield. The RC of *Rhodobacter sphaeroides* consists of three subunits, called L, M, and H. The former two subunits harbor four BChls (P_L, P_M, B_A, and B_B), two BPhs (Φ_A and Φ_B), two ubiquinones (Q_A and Q_B), and one carotenoid molecule together with one non-heme iron as cofactors (*1*, *2*). The cofactors form two branches with an approximate *C2* symmetry (Figure 1). Upon light excitation the singlet excited-state P* of the primary donor, a dimer of the two BChls P_L and P_M, is formed and an electron is transferred from P via the cofactors in the so-called A-branch, B_A, Φ_A,

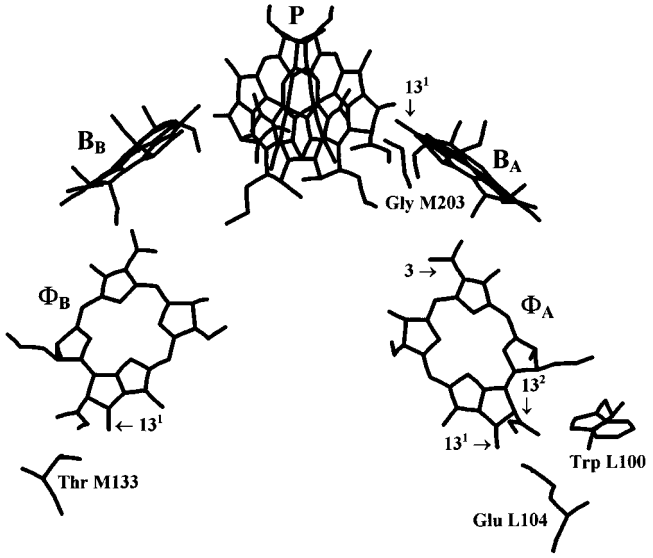

FIGURE 1: Structural arrangement of the bacteriochlorin cofactors and the native amino acid residues at positions L100, L104, M133, and M203 in wild-type RCs of *R. sphaeroides* according to the X-ray structure analysis (*2*): P, BChls of the primary donor; B_A, B_B, accessory BChls; Φ_A, Φ_B, BPhs. The 13^1-keto groups of B_A, Φ_A, and Φ_B as well as the 3-acetyl group and the 13^2-methyl ester of Φ_A are indicated. For clarity, the phytyl chains are truncated, and the quinone acceptors, the non-heme iron, and the carotenoid molecule are not shown.

† This work was supported by DFG (Sfb 312, TP A4), Fonds der Chemischen Industrie to W.L., USDA (97-3503-4524) to J.C.W., and NaFöG to F.M.

* To whom correspondence should be addressed.

‡ Technische Universität Berlin.

§ Arizona State University.

[1] Abbreviations: θ, dihedral angle; $\Phi_{A,B}$, BPh in the A- and B-branch, respectively (also referred to in the literature as $H_{A,B}$ or $H_{L,M}$); A, hfc constant; A_{eff}, effective hfc constant; A_{iso}, isotropic hfc constant; $A_\perp$, $A_{||}$, perpendicular and parallel components of uniaxial hf tensor; BChl, bacteriochlorophyll; BPh, bacteriopheophytin; Brij 36 T, lauryldecaoxyethylene-ether; cyt, cytochrome; ENDOR, electron nuclear double resonance; EPR, electron paramagnetic resonance; ET, electron transfer; I, intermediate acceptor; hf(c), hyperfine (coupling); LDAO, *N*-lauryl-*N*,*N*-dimethylamine-*N*-oxide; LUMO, lowest unoccupied molecular orbital; MO, molecular orbital; OR, optical ratio; P, primary donor; $Q_{A,B}$, primary and secondary quinones, respectively; $Q_{x,y}$, optical transitions in BChls and BPhs; RC, reaction center; rf, radio frequency; RHF-INDO/SP, restricted Hartree−Fock intermediate neglect of differential overlap/spin polarization; SB14, *N*-(*n*-tetradecyl)-*N*,*N*-dimethyl-3-ammonio-1-propanesulfonate; TE, Tris/EDTA buffer; TRIPLE, electron nuclear nuclear triple resonance; Triton X-100, *tert*-octylphenylpolyoxyethylene-ether.

S0006-2960(98)00799-5 CCC: $15.00
Published on Web 09/01/1998

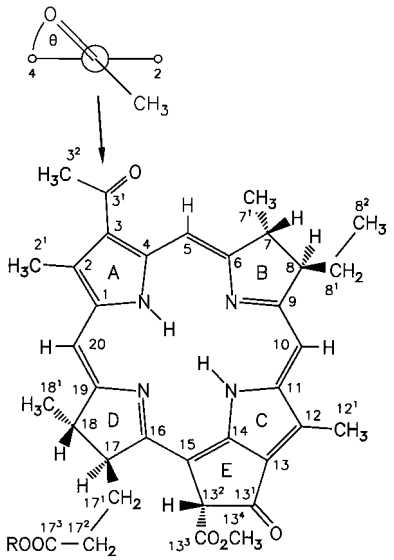

FIGURE 2: Structure of BPh *a* with IUPAC numbering scheme (R = phytyl). The dihedral angle θ defining the orientation of the 3-acetyl group is given. The arrow indicates the viewing direction along the C3−C3^1 bond axis.

and Q_A, to the terminal acceptor Q_B (*3*). Despite the quasi-symmetric arrangement of potential electron carriers no ET along the B-branch is observed in wild-type RCs.[2]

At ambient temperatures the state $P^{\bullet+}\Phi_A^{\bullet-}$ is formed in ~4 ps after excitation of P, and the electron is further transferred to Q_A in ~200 ps. At low temperatures the optical Q_x transitions of Φ_A and Φ_B can be clearly distinguished with absorption maxima at 546 and 534 nm, respectively. It has been shown by site-directed mutagenesis that the main reason for this bandshift is a hydrogen bond between glutamic acid (Glu) L104 and the 13^1-keto group of Φ_A (for numbering, see Figure 2), although it is not the only origin of differences between the optical properties of the two BPhs (*5*−*9*). Transient optical spectroscopy revealed the unidirectionality of the ET by showing that only the long-wavelength Q_x band is bleached upon formation of the $P^{\bullet+}\Phi_A^{\bullet-}$ state (*10*, *11*).

A similar selective bleaching at 546 nm is observed when the steady-state $I^{\bullet-}$ is formed, which therefore is assigned to $\Phi_A^{\bullet-}$. In the case of *R. sphaeroides* this state can be accumulated by illumination of RCs with actinic light in the presence of a strong reductant (sodium dithionite) and a soluble secondary electron donor (native cyt c_2 or cyt *c* from horse heart). As has been shown by Okamura et al. (*12*) the trapping of $I^{\bullet-}$ occurs in three steps. First, after chemical reduction of the quinone acceptors, illumination in the presence of cyt yields the state $I^{\bullet-}Q_A^{\bullet-}$. In a second dark reaction the diamagnetic state IQ_A^{2-} is formed. A final light reaction then yields $I^{\bullet-}Q_A^{2-}$. Alternatively, the state $I^{\bullet-}$ can be obtained directly in quinone-depleted RCs. The halftime of $I^{\bullet-}$ in the absence of oxygen at room temperature is only 15−20 min, but the radical anion is stable at temperatures below 200 K.

[2] So far, evidence for ET to Φ_B (~15%) was only found in one site-directed mutant of RCs from *Rhodobacter capsulatus*, in which the photoactive BPh was replaced by a BChl through the introduction of His at position M212 and, in addition, Gly at position M201 was replaced by Asp (*4*).

Characterization of $I^{\bullet-}$ using optical spectroscopy is hampered by difficulties in interpreting the $I^{\bullet-}$/I difference spectra (*12*−*15*). In particular, there is a strong bleaching and shift of the BChl Q_y band at 805 nm, making the assignment of the observed changes to the formation of a BPh *a* anion problematical. More specific information can be obtained through investigation of the electronic structure of $I^{\bullet-}$ using EPR methods such as ENDOR or Special TRIPLE resonance. By these methods the hfc's of the unpaired valence electron of $I^{\bullet-}$ with certain magnetic nuclei can directly be measured (*16*−*19*).

Investigation of the electron spin density distribution of $I^{\bullet-}$ in RCs from *R. sphaeroides* led to the identification of this state with a monomeric BPh or BChl radical anion (*20*−*24*). The observed hfc's were, however, somewhat different from those of the respective anions in organic solvents, which was attributed to the interaction of the reduced cofactor with its protein environment (*18*). Removal of the hydrogen bond between Glu L104 and the 13^1-keto group of Φ_A resulted in a significant change of the electronic structure of $I^{\bullet-}$ (vide infra) and finally gave evidence that the trapped species is the BPh radical anion on the A-branch (*8*).

Here we show by ENDOR and Special TRIPLE spectroscopy that (at least) two distinct $I^{\bullet-}$ states can be freeze-trapped in RCs from *R. sphaeroides*, depending on the trapping conditions and the temperature. To assign these states to a certain cofactor we also examined site-directed mutants with specific changes near the bacteriochlorins. Two mutants, EL(L104), in which the above-mentioned Glu at position L104 (L-subunit) is replaced by Leu, and WF(L100), in which Trp at position L100 is exchanged to Phe, were designed to remove putative hydrogen bonds to Φ_A (Figure 1). The effects of these mutations on the electronic structure of the two $I^{\bullet-}$ states are discussed. Also investigated are TD(M133), in which Thr at position M133 is replaced by Asp in order to introduce a hydrogen bond to the 13^1-keto group of Φ_B (Figure 1), and the double mutant EL-(L104)+TD(M133). In addition, we examined the $I^{\bullet-}$ state in the mutant GD(M203), in which Gly at position M203 near the 13^1-keto group of B_A is replaced by Asp (*25*). The results from all of the mutants allow us to identify the two $I^{\bullet-}$ states with different conformations of $\Phi_A^{\bullet-}$. The reasons for the occurrence of these conformations and possible implications for the initial charge separation process are discussed.

MATERIALS AND METHODS

The construction of mutants using oligonucleotide-directed mutagenesis has been described earlier (*9*, *25*). All mutant strains were able to grow photosynthetically. RCs were isolated from semi-anaerobically grown wild-type and mutant cells following published procedures (*26*, *27*). The wild-type RCs were those of the ΔLM1.1 deletion strain complemented with wild-type genes. The buffer used throughout (TE) contained 10 mM Tris/HCl (pH 8.0) and 1 mM EDTA. Detergent exchange was performed either by dialysis or by washing RCs bound to a DEAE column (Fractogel TSK 650 S, Merck) and eluting with 300 mM NaCl. After desalting the RC solutions were concentrated to $OD_{805} \approx 100$ (Centricon 30, Amicon) and stored at 200 K. Detergents were purchased from Fluka (LDAO, Triton X-100) and

Sigma (Brij 36T, SB14). RC concentrations were determined optically by using the molar extinction coefficient $\epsilon_{805} = 2.88\ mM^{-1}\ cm^{-1}$ (*28*).

The quinone content of RCs was assayed photochemically according to Okamura et al. (*29*) using horse heart cyt *c* (Sigma). Quinone extraction was performed by washing RCs bound to a DEAE column overnight at room temperature with 10 mM *o*-phenanthroline and 1% (w/v) Brij 36 T in TE (1 L of washing buffer/10 in.). Excess detergent and *o*-phenanthroline were then removed by washing with 0.1% (w/v) Brij 36 T in TE and RCs eluted with 300 mM NaCl. The obtained RCs contained only ~1% Q_A as judged from the amplitude of the flash-induced $P^{\bullet+}Q_A^{\bullet-}$ signal.

Cyt c_2 was isolated from the supernatant of the chromatophore preparation following the method of Axelrod et al. (*30*) with modifications. After removal of membrane fragments, soluble proteins were precipitated with $(NH_4)_2SO_4$ to 30% saturation at pH 7.3, and the supernatant was applied to a hydrophobic column (*n*-butyl-Sepharose fast flow, Pharmacia) equilibrated in TE (pH 7.3) containing $(NH_4)_2SO_4$ to 30% saturation. Fractions of eluting buffer that contained cyt c_2 were pooled, adjusted to 60% saturated $(NH_4)_2SO_4$, and centrifuged (8000 g, 45 min). The supernatant was applied to a second hydrophobic column equilibrated with 60% saturated $(NH_4)_2SO_4$, the bound proteins washed extensively with equilibrium buffer, and eluted with 40% saturated $(NH_4)_2SO_4$. Cyt c_2 fractions with an $OR_{280/416} \approx 0.25$ were obtained. The pooled fractions were dialyzed against TE (pH 7.3) and concentrated by putting the dialysis tubing on PEG 3350 (Sigma) overnight at 278 K. The concentrated solution was dialyzed three times against TE (pH 7.3) containing 1 mM sodium ascorbate in the first two steps. The $(NH_4)_2SO_4$-free solution was applied to a DEAE column equilibrated in TE (pH 7.3). Bound cyt c_2 was washed with equilibrium buffer and eluted with 100 mM NaCl to give $OR_{280/416} \approx 0.22$. After dialysis against TE (pH 8.0), the protein was concentrated to $OD_{550} \approx 150$ (Centricon 10, Amicon) and stored at 200 K.

Optical spectroscopy at room and cryogenic temperatures was performed using a Cary 5 spectrophotometer (Varian) as described earlier (*25*). The EPR, ENDOR, and Special TRIPLE measurements were performed on a Bruker ESP 300E spectrometer with a home-built cavity and radio frequency accessories that are described in detail elsewhere (*31*, *32*). Typical samples were 90 μL of a solution containing 120−140 μM RC and 0.5−2.0 mM cyt c_2 in 0.1% (w/v) Triton X-100 or 0.1% (w/v) Brij 36T in TE (pH 8.0) that was mixed with 10 μL of a freshly prepared 0.5 M $Na_2S_2O_4$ solution in 1 M Tris/HCl (pH 8.0) in an argon-flushed glass tube (i.d. 3 mm). To prevent glass breakage through freezing, a piece of Teflon tubing, which was sealed on the bottom, was inserted into the sample. Samples were illuminated in an ice−water bath for 1 or 45 s with white light using a 150 W halogen lamp before rapid freezing in liquid nitrogen. The illumination was continued during the freezing process, but not during the subsequent measurement. H/D exchange was performed by repeated cycles of diluting samples with D_2O containing 0.05% (w/v) Triton X-100 and reconcentrating them in centricon 30 tubes (Amicon), followed by incubation for 70 h at room temperature prior to the $I^{\bullet-}$ accumulation.

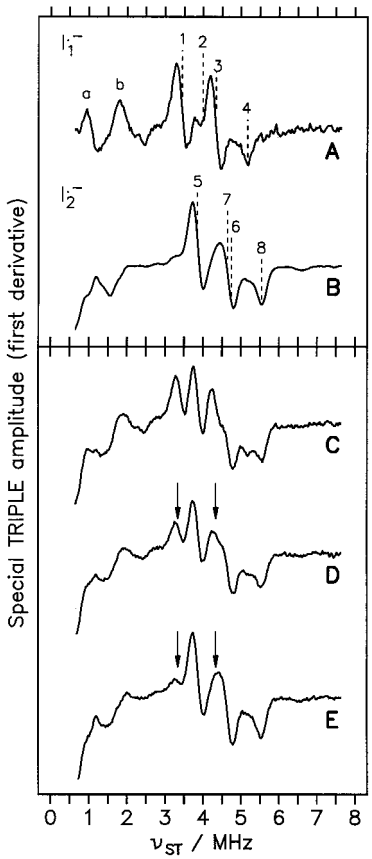

FIGURE 3: ^{1}H-Special TRIPLE spectra of the two freeze-trapped $I^{\bullet-}$ states, $I_1^{\bullet-}$ and $I_2^{\bullet-}$ (A and B), in wild-type RCs from *R. sphaeroides* (detergent 0.1% Triton X-100). $I_2^{\bullet-}$ is obtained at 160 K with 45 s illumination prior to freezing (B). $I_1^{\bullet-}$ is obtained together with $I_2^{\bullet-}$ with 1 s illumination, measured at 135 K (C). Its intensity decreases at higher temperatures (see, D, 150 K; E, 165 K). The difference spectrum (A) is obtained from the two spectra in C and E. Note that the spectrum in B contains small contaminations from the $I_1^{\bullet-}$ state. For assignment and hfc's of the signals 1−8, see text and Table 1. Arrows in C to E indicate the irreversible decay of signals 1 and 3 ($A_\perp$ components) assigned to $I_1^{\bullet-}$. The additional signals a and b (in A) have effective hfc's of $A_{eff}(a) \approx 2.0$ MHz and $A_{eff}(b) \approx 4.0$ MHz. Experimental conditions: microwave power 12 mW, rf power 2 × 100 W, rf modulation depths 140 kHz (frequency 12.5 kHz), time constant 326 ms (1024 datapoints, 30 scans).

RESULTS

Electronic Structure of $I^{\bullet-}$ in Wild Type. The X-band EPR signal of the freeze-trapped state $I^{\bullet-}Q_A^{2-}$ in wild-type RCs from *R. sphaeroides*, accumulated with 45 s illumination prior to freezing, is an inhomogeneously broadened Gaussian line with a width of $\Delta B_{pp} = 1.29 \pm 0.03$ mT (not shown), which is typical for a BPh *a* (or BChl *a*) radical anion (*18*, *26*). The proton hfc constants *A* can be obtained from ^{1}H-ENDOR or Special TRIPLE spectroscopy[3] (*16*−*19*). The main feature of the Special TRIPLE spectrum (Figure 3B) is two overlapping uniaxial hf tensors (signals 5−8) with

[3] The ^{1}H-Special TRIPLE resonance frequencies ν_{ST} are related to the hfc constants *A* by $\nu_{ST} = |\nu^{\pm}_{ENDOR} - \nu_H| = |A|/2$, if the ENDOR resonance frequencies are to first order symmetrically spaced around the proton Larmor frequency ν_H in the applied magnetic field (*19*). We found no differences between hf tensor components when they were determined from either ENDOR or Special TRIPLE spectra, indicating that at least for the methyl hfc's any deviation from the symmetry around ν_H is less than the experimental error of ~±100 kHz.

Table 1: ^{1}H-hfc Tensor Components (MHz), Isotropic hfc's, Sums and Ratios of hfc's of the 2^1 and 12^1 Methyl Protons of the Two $I^{\bullet-}$ States in Native and Mutant RCs from *R. sphaeroides* and of the Radical Anions of BPh *a* and BChl *a* in Frozen Organic Solution

assignment to state	$I_1^{\bullet-}$								$I_2^{\bullet-}$							
assignment to molecular position [a]	2^1			12^1			Σ [f]	R [g]	2^1			12^1			Σ [f]	R [g]
assignment to tensor components	$A_\perp$	$A_\parallel$	A_{iso} [e]	$A_\perp$	$A_\parallel$	A_{iso} [e]			$A_\perp$	$A_\parallel$	A_{iso} [e]	$A_\perp$	$A_\parallel$	A_{iso} [e]		
signal number	1	2		3	4				5	6		7	8			
R. sphaeroides [b]																
wild type	6.7	7.9	7.1	8.4	10.3	9.0	16.1	1.27	7.5	9.3 [i]	8.1	9.0 [i]	11.0	9.7	17.8	1.20
wild type, q.d.	6.6	8.1	7.1	8.5	10.4	9.1	16.2	1.28	7.7	9.4 [i]	8.3	9.1 [i]	11.0	9.7	18.0	1.17
EL(L104)	n.d. [h]			n.d. [h]			-	-	6.3	7.9	6.8	9.5	11.4	10.1	16.9	1.49
EL(L104), q.d.	7.0	8.8	7.6	9.7 [i]	11.7 [i]	10.4 [i]	18.0 [j]	1.37 [k]	6.1	7.7	6.6	9.4 [i]	11.4 [i]	10.1 [i]	16.7 [j]	1.53 [k]
WF(L100)	n.d. [h]			n.d. [h]			-	-	7.2	8.7	7.7	9.2	11.1	9.8	17.5	1.27
WF(L100), q.d.	6.7	7.8	7.1	8.2	10.0	8.8	15.9	1.24	7.2	8.7	7.7	9.1	11.1	9.8	17.5	1.27
GD(M203)	n.d. [h]			n.d. [h]			-	-	7.5	9.3 [i]	8.1	8.9 [i]	10.9	9.6	17.7	1.19
TD(M133)	n.d. [h]			n.d. [h]			-	-	7.5	9.3 [i]	8.1	9.0 [i]	11.0	9.7	17.8	1.20
EL(L104)+TD(M133)	n.d. [h]			n.d. [h]			-	-	6.3	7.9	6.8	9.5	11.4	10.1	16.9	1.49
BPh a^-																
pyr/H_20 [c]	-	-	-	-	-	-	-	-	7.1	8.6	7.6	8.4	10.1	9.0	16.9	1.18
MTHF [d]	-	-	-	-	-	-	-	-	7.1	8.2	7.5	8.2	10.0	8.8	16.3	1.17
BChl a^-																
pyr/H_20 [c]	-	-	-	-	-	-	-	-	8.7	10.1	9.2	10.1	12.1	10.8	20.0	1.17
MTHF [d]	-	-	-	-	-	-	-	-	8.0	9.2	8.4	9.2	11.1	9.8	18.2	1.17

[a] For numbering see Figure 2. [b] Both $I^{\bullet-}$ states are obtained with 1 s illumination prior to freezing ($T = 135$ K); $I_2^{\bullet-}$ is accumulated preferentially with 45 s or longer illumination prior to freezing ($T = 135-180$ K); the hf tensor components are obtained from simulations of difference spectra (cf. Figure 3); q.d., quinone depleted (cf. Materials and Methods); same values for 0.1% Triton X-100 (*tert*-octylphenyl polyoxyethylene ether) and 0.1% Brij 36 T (*n*-dodecyl decaoxyethylene ether); error of tensor components, ±100 kHz. [c] Aqueous pyridine, $T = 145$ K (*23*). [d] 2-Methyl tetrahydrofuran, $T = 100$ K (*23*). [e] Isotropic hfc's, $A_{iso} = (2A_\perp + A_\parallel)/3$; error, ±100 kHz. [f] $\Sigma = A_{iso}(2^1) + A_{iso}(12^1)$; error, ±200 kHz. [g] $R = A_{iso}(12^1)/A_{iso}(2^1)$; error, ±0.02. [h] n.d., not determined. [i] Error of this hfc, ±200 kHz. [j] Error, ±400 kHz. [k] Error, ±0.04.

the tensor components $A_\perp$ (signals 5 and 7) and $A_\parallel$ (signals 6 and 8; $A_\parallel > A_\perp > 0$) and the (positive) isotropic hfc $A_{iso} = (2A_\perp + A_\parallel)/3$, which are assigned to the protons of the two methyl groups at positions 2^1 and 12^1 (Table 1). The principal hf tensor components are deduced from simulations of the powder pattern (*33*).

The methyl signals are accompanied by smaller broad signals in the range of $\nu_{ST} = 2-7$ MHz. These can be assigned to the α-protons at positions 5, 10, and 20 (not labeled in Figure 3), since these protons are expected to have large and strongly anisotropic hfc's in the BPh *a* radical anion (*18*). The unambiguous assignment of the tensor components of these signals in frozen solution is difficult because of their weak intensity and will not be further discussed here. However, it should be kept in mind that these tensor components may be superimposed to the methyl signals and could cause some distortions of the line shapes.

The EPR and Special TRIPLE spectra of $I^{\bullet-}$ obtained with 45 s of illumination prior to freezing in liquid nitrogen (cf. Materials and Methods) are insensitive to the temperature between 135 and 180 K. However, when the illumination time is decreased to 1 s and the measurement is performed at 135 K, the line width of the EPR signal is reduced to $\Delta B_{pp} = 1.21 \pm 0.03$ mT (not shown). The pattern of intense narrow lines in the corresponding Special TRIPLE spectrum is significantly changed (Figure 3C). Variation of the temperature without further illumination reveals that the intensity of certain lines (in particular, signals 1 and 3) is strongly decreased upon warming the sample to 165 K (see arrows in Figure 3). This is accompanied by an increase of the EPR line width to a value similar to that obtained with 45 s illumination. Further increase of the temperature to 180 K results in no additional changes. Likewise the EPR and Special TRIPLE spectra remain unaltered upon recooling the sample within the cavity to 135 K in the dark, indicating that the observed changes are *irreversible*.

The Special TRIPLE spectra obtained between 135 and 165 K with 1 s illumination can be interpreted by the presence of two distinct spectroscopic species. We call these species $I_1^{\bullet-}$ and $I_2^{\bullet-}$ (cf. Figure 3A,B). Obviously, $I_1^{\bullet-}$ is metastable and decays between 135 and 160 K, while $I_2^{\bullet-}$ is stable under these conditions ($T < 200$ K). The spectrum of $I_2^{\bullet-}$ is identical to that obtained with 45 s illumination (Figure 3B). The spectrum of the pure $I_1^{\bullet-}$ state (Figure 3A) can be obtained by subtracting the spectrum measured at 165 K (Figure 3E) from that at 135 K (Figure 3C). The difference spectrum exhibits two somewhat different uniaxial hfc tensors (signals 1−4) with different isotropic hfc's (Table 1). These are assigned to methyl protons as indicated (cf. Discussion). In addition, there are two signals, labeled a and b (Figure 3A), with effective hfc's of $A_{eff}(a) \approx 2.0$ MHz and $A_{eff}(b) \approx 4.0$ MHz. These signals are not present or are at least much weaker in the spectrum of $I_2^{\bullet-}$ and are probably superimposed to other resonances in the range $\nu_{ST} \leq 2$ MHz.

To assess a possible involvement of the primary quinone acceptor in the formation of the metastable state $I_1^{\bullet-}$ we

repeated the experiments described above with quinone-depleted RCs. With 1 s illumination both states $I_1^{\bullet-}$ and $I_2^{\bullet-}$ are present at 135 K (not shown), exhibiting essentially the same hfc's as observed with quinone containing RCs[4] (Table 1). Here, the $I_1^{\bullet-}$ state also relaxes irreversibly upon warming the sample to 180 K. The replacement of Triton X-100 by Brij 36T, which was used for quinone extraction, caused no changes of hfc's.

To obtain information about the origin of the two signals a and b of $I_1^{\bullet-}$ we investigated RCs that were incubated in D_2O for 70 h prior to the $I^{\bullet-}$ accumulation (cf. Materials and Methods). Under these conditions both signals are clearly present with the same spectral intensity as in H_2O. Further experiments were performed on RCs of *R. sphaeroides* R26.1 isolated from cells that were grown on D_2O medium with succinic acid-h_4 as the sole proton source (*37*, *38*). In these preparations the bacteriochlorins are deuterium labeled at positions 5, 7, 8, 8^1, 8^2, 10, 17, 17^1, 17^2, 18, and 20 and partially at position 13^4 and at the phytyl chain (Figure 2). Protons are only fully retained at positions 2^1, 3^2, 7^1, 12^1, 13^2 (exchangeable), and 18^1. The signals a and b were essentially absent under these conditions.

Characterization of Mutants by Optical Spectroscopy. The room temperature optical absorption spectra (not shown) of the isolated RCs from all mutants were not significantly different from that of the wild type, with the exception of the mutants with the change Glu to Leu at position L104, in which the Q_x band of the BPhs was substantially narrowed.

In the low-temperature (20 K) optical spectra of the mutants with changes near the BPhs, shifts of bands are only observed in the BPh Q_x region (not shown). In the case of the mutant EL(L104) the spectrum shows one asymmetric peak at 536 nm, which is similar to the one in the mutant EV(L104) (*6*) and the *Rhodobacter capsulatus* mutant EL-(L104) (*5*). The spectrum of TD(M133) contains a peak at 546 nm and a shoulder at ~540 nm as compared with the two peaks at 546 and 534 nm in the wild type. In the corresponding spectrum of the double mutant EL(L104)+TD-(M133) only one peak at 537 nm is observed. The mutant WF(L100) shows two peaks quite similar to those of the wild type, but there are small changes in amplitudes and line widths. The spectrum of the mutant GD(M203) with a change near B_A has been published earlier (*25*). In contrast to the other cases, band shifts are seen here only in the BChl Q_x and Q_y region. The observed changes are consistent with the assumption that the point mutations have specific local effects on the spectral properties of nearby cofactors and are additive, for example, in the double mutant. In addition, the overall structure and pigment composition of the RCs seems to be not affected by these mutations.

[4] A slight blue shift of the long wavelength band of the primary donor P from 866 to ~863 nm is observed in Brij 36 T upon quinone depletion of RCs (cf. ref *34*), which can be interpreted in terms of a detergent-induced conversion of ~20% of the RCs to the so-called P_{850} state. A shift to 851 ± 1 nm corresponds to 100% conversion (*35*, *36*). To assess possible effects on the electronic structure of $I^{\bullet-}$ we also investigated this anion in RCs in the P_{850} state induced by solubilization with the zwitterionic detergent SB14. The observed hf tensors of the two methyl groups 2^1 and 12^1 in the state $I_2^{\bullet-}$ (freeze-trapped with 45 s illumination prior to freezing) are only slightly shifted ($A_{iso}(2^1)$ = 7.9 MHz, $A_{iso}(12^1)$ = 9.9 MHz, Σ = 17.8 MHz, R = 1.25) compared with samples in nonionic detergents (Table 1). There are no indications for a preferential formation of the $I_1^{\bullet-}$ state under these conditions.

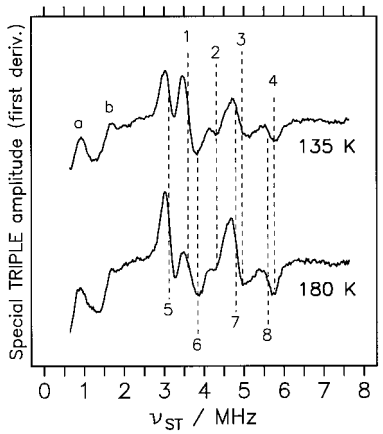

FIGURE 4: ^{1}H-Special TRIPLE spectra of freeze-trapped $I^{\bullet-}$ in quinone-depleted RCs of the *R. sphaeroides* mutant EL(L104), recorded at two different temperatures (illumination time 1 s, detergent 0.1% Brij 36T). For assignment and hfc's of the signals 1−8, see text and Table 1. Note the (irreversible) decay of signal 1 ($A_\perp$ component) assigned to $I_1^{\bullet-}$. The additional signals a and b have effective hfc's of A_{eff}(a) ≈ 2.0 MHz and A_{eff}(b) ≈ 4.0 MHz. For experimental conditions, see Figure 3.

Electronic Structure of $I^{\bullet-}$ in Mutant RCs. With 1 s illumination prior to freezing, two distinct $I^{\bullet-}$ states are also observed in quinone-depleted RCs of the mutant EL(L104). As in the case of the wild type, one can identify four uniaxial hf tensors (Figure 4), two of which lose spectral intensity irreversibly upon increasing the temperature from 135 to 180 K. The principal hf tensor components are again obtained from simulations of difference spectra (not shown). This allows an assigment of the signals 1−4 to the metastable state $I_1^{\bullet-}$ and of the signals 5−8 to $I_2^{\bullet-}$. The signals belonging to position 12^1, that is, 3 and 7 as well as 4 and 8, respectively, are the same within the experimental error (cf. Table 1). The hfc's assigned to position 2^1 are, however, different in the two $I^{\bullet-}$ states. As compared with the wild type the isotropic hfc's for the methyl groups at positions 2^1 and 12^1 are significantly different in the mutant (Table 1). In particular, there is a strong decrease of $A_{iso}(2^1)$ and a slight increase of $A_{iso}(12^1)$ in both states, $I_1^{\bullet-}$ and $I_2^{\bullet-}$. The two signals a and b of $I_1^{\bullet-}$ have only weak intensity. In quinone-containing RCs of EL(L104) a sufficient signal-to-noise ratio of the Special TRIPLE spectra was obtained only with illumination of 45 s or longer prior to freezing (spectra not shown). The observed methyl hfc's are essentially the same as those of $I_2^{\bullet-}$ in quinone-depleted RCs (Table 1).

As is evident from Figure 5, two distinct $I^{\bullet-}$ states can also be trapped under the same experimental conditions in RCs of the mutant WF(L100). The hfc's of $I_1^{\bullet-}$, including the two uniaxial hf tensors of the methyl protons (signals 1−4) as well as the additional signals a and b, are quite similar to that of $I_1^{\bullet-}$ in the wild type. The methyl hf tensors of $I_2^{\bullet-}$ (signals 5−8) are changed such that the ratio R = $A_{iso}(12^1)/A_{iso}(2^1)$ is increased (Table 1) and the components of both methyl hf tensors are fully resolved (in particular, signals 6 and 7). Two signals with A_{eff} ≈ 2.0 MHz and A_{eff} ≈ 4.0 MHz similar to the signals a and b of $I_1^{\bullet-}$ are also observed with 45 s illumination in quinone-containing RCs.

The ENDOR and Special TRIPLE spectra of $I^{\bullet-}$ in the mutants GD(M203) and TD(M133), freeze-trapped with 45 s illumination and measured at 160 K, show no significant shifts of the methyl hfc's as compared with $I_2^{\bullet-}$ in the wild

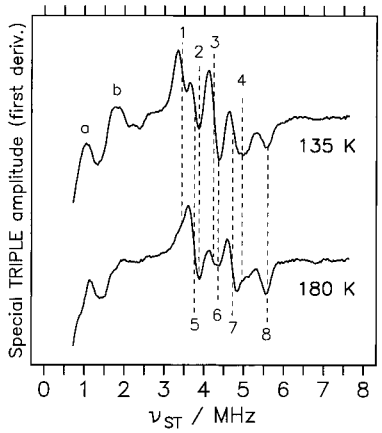

FIGURE 5: ^{1}H-Special TRIPLE spectra of freeze-trapped $I^{\bullet-}$ in quinone-depleted RCs of the *R. sphaeroides* mutant WF(L100), recorded at two different temperatures (illumination time 1 s, detergent 0.1% Brij 36T). For assignment and hfc's of the signals 1−8, see text and Table 1. Note the (irreversible) decay of signals 1 and 3 ($A_\perp$ components) assigned to $I_1^{\bullet-}$. The additional signals a and b have effective hfc's of A_{eff}(a) ≈ 2.0 MHz and A_{eff}(b) ≈ 4.0 MHz. For experimental conditions, see Figure 3.

type (Table 1, spectra not shown). In the spectra of both mutants traces of signals can be detected that are similar to the methyl hfc's of $I_1^{\bullet-}$ in the wild type as observed at 165 K (cf. Figure 3E). There is no evidence for additional spectroscopic species that, for example, could originate from a (partial) reduction of B_A or Φ_B. The methyl hfc's seen in the ENDOR spectrum of the double mutant EL(L104)+TD-(M133) are similar to those of the single mutant EL(L104) as would be expected, if the additional mutation at position M133 has no influence on the electronic structure of $I^{\bullet-}$ (Table 1, spectra not shown). Two signals with $A_{eff} \approx 2.0$ MHz and $A_{eff} \approx 4.0$ MHz are observed with 45 s illumination or longer (i.e., up to 2 min) in the ENDOR spectra of $I^{\bullet-}$ in quinone-containing RCs of GD(M203) and EL(L104)+TD-(M133) similar to the case of WF(L100). If these hfc's correspond to the signals a and b in $I_1^{\bullet-}$ of the wild type (cf. Figure 3A), then their spectral intensity is apparently not strongly correlated with the presence of this state in the mutants.

DISCUSSION

Assignment of hfc's and Identification of Two $I^{\bullet-}$ States in RCs of R. sphaeroides. The assignment of the intense signals 1−8 observed in ENDOR and Special TRIPLE spectra of $I^{\bullet-}$ in frozen solution to methyl protons is based on the fact that in polycrystalline samples only the methyl groups show intense narrow ENDOR signals due to their rapid rotation and symmetry (*16*, *39*). The further assignment to specific methyl groups (positions 2^1 or 12^1) is based on a comparison with semiempirical calculations (RHF-INDO/SP) discussed below.

The occurrence of isotropic hf interactions due to protons of methyl groups adjacent to the π-system can be explained by *hyperconjugation* (*40*). The observed proton hfc $A_{iso}(X^1)$ of a methyl group is proportional to the π-spin density (*41*, *42*) and can therefore be used as a direct measure of the π-spin density at carbon X, for example, at positions 2 or 12 (Figure 2). ENDOR studies of BPh $a^{\bullet-}$ and BChl $a^{\bullet-}$ in organic solution showed that the π-spin density at the methyl positions yields a sum of methyl hfc's lying in the range of $\sum$ = 16−17 MHz and 18−20 MHz, respectively, for the monomeric radical anions (*16*, *23*). Furthermore, it is usually found that $A_{iso}(2^1) < A_{iso}(12^1)$, resulting in a characteristic ratio of methyl hfc's of $R = A_{iso}(12^1)/A_{iso}(2^1) \approx 1.2$. The values for $I^{\bullet-}$ obtained with an illumination of 45 s or longer fall into this range, indicating that the trapped species is a *monomeric* bacteriochlorin radical anion (Table 1). The spectra obtained with short illumination (1 s) show two additional methyl hf tensors, which lose intensity with increasing temperature between 135 and 160 K. Since the amplitudes of the Special TRIPLE resonances are not expected to be as sensitive to temperature as those of ENDOR (*43*), it follows that the two additional methyl signals must be ascribed to a second distinct radical, the *population* of which is temperature-dependent. The sum $\sum$ and ratio R of the methyl hfc's allow this second radical to be also identified with a *monomeric* bacteriochlorin radical anion (Table 1).

Experiments on RCs from bacteria grown on D_2O media together with the analysis of the isotopic composition of pigments isolated from such samples by NMR spectroscopy (*37*, *38*) allow a further assignment of the measured hfc's. In spectra of such partially deuterium labeled samples, the methyl signals of both $I^{\bullet-}$ states are clearly present under the respective illumination conditions. This is expected from the isotopic composition, since the methyl positions 2^1 and 12^1 are protonated. The two additional signals a and b of the $I_1^{\bullet-}$ state, however, are no longer observed. Note that in normal wild-type RCs (grown on H_2O) the intensity of these two signals with respect to that of the methyl protons in the $I_1^{\bullet-}$ state does not vary significantly between different samples, even if the RCs are incubated in D_2O (cf. Results). Therefore, the disappearance of these signals indicates that the corresponding molecular positions are deuterated and do not belong to exchangeable protons (cf. ref *24*). Among the possible positions (cf. Results) only the β-protons at carbons 7 and 8 or 17 and 18 of the saturated rings B and D are expected to have relatively large hfc's with low anisotropy as observed in the spectra (*18*, *44*). The isotropic hfc's of these protons depend not only on the π-spin density but also on the angle between the axis perpendicular to the π-system and the CH-bond axis (*41*, *42*). It is possible that a conformational change of the saturated ring alters the β-proton hfc's without strongly affecting the π-spin density distribution. Therefore, the intensity, width, and effective hfc constant of these signals can vary significantly between states as compared with the signals of the methyl protons. This could explain why the amplitudes of the signals a and b are large in the $I_1^{\bullet-}$ state, but negligible in the $I_2^{\bullet-}$ state. On the basis of these arguments, we assign the signals a and b tentatively to β-protons at the saturated rings.

Assignment of the Two $I^{\bullet-}$ States to $\Phi_A^{\bullet-}$. A clear assignment of the identified bacteriochlorin radical anions to specific cofactors is not possible based on the wild-type data only. To exclude the possibility that the unpaired electron is trapped on cofactors other than Φ_A (e.g., on Φ_B or B_A), we investigated mutant RCs with specific alterations in the vicinity of certain cofactors. The two mutants EL-(L104) and WF(L100) were constructed to remove putative hydrogen bonds between Φ_A and its protein environment (Figure 1). In the mutants *both* states, $I_1^{\bullet-}$ and $I_2^{\bullet-}$, are

affected, although $I_1^{\bullet-}$ in WF(L100) is quite similar to $I_1^{\bullet-}$ in the wild type. Further insight comes from the observation that mutations in the vicinity of other cofactors have no significant effect on the electronic structure of $I^{\bullet-}$. The mutants GD(M203) and TD(M133) were constructed to introduce a hydrogen bond to the 13^1-keto group of B_A and Φ_B, respectively. Although we have no clear evidence for the formation of such hydrogen bonds in these mutants, the optical spectra show that the respective cofactors are perturbed by the nearby mutations in a manner similar to the effects of the hydrogen bond to Φ_A. Consequently, measurable effects on the electronic structure of $I^{\bullet-}$ in these mutants should be expected, if the electron was trapped on B_A or Φ_B. However, no effects are observed. In addition, the changes due to the double mutant EL(L104)+TD(M133) are the same as those due to the single mutant EL(L104). We therefore conclude that the electron is selectively trapped on Φ_A, and that the unidirectionality of the ET is not affected by the investigated mutations. This assignment implies that the two $I^{\bullet-}$ states must be interpreted as different conformations of the same radical anion, $\Phi_A^{\bullet-}$.

MO Calculations of hfc's. Semi-empirical molecular orbital calculations have been used extensively to obtain a detailed understanding of the spin density distribution in the frontier orbitals of bacteriochlorin radical cations and anions and have proven to be a valuable tool for the interpetation of ENDOR and Special TRIPLE spectra (*18*, *33*, *44*, *45*). Of particular importance for the assignment of the methyl hfc's of BPh $a^{\bullet-}$ is the dependence of the s-spin densities at positions 2^1 and 12^1 on the torsional motion of the 3-acetyl group. RHF-INDO/SP calculations of the total energy and the spin density distribution within the LUMO of BPh $a^{\bullet-}$ *in vacuo* as a function of the dihedral angle θ (cf. Figure 2) revealed that the total energy has two minima at $\theta \approx 45°$ and 135° that are separated by a small barrier at $\theta \approx 90°$. The barrier is probably caused by a decrease of the conjugation between the acetyl group and the π-system of the macrocycle. An in-plane orientation of the 3-acetyl group of BPh $a^{\bullet-}$ *in vacuo* is clearly not favored, since the total energy rises strongly due to steric hindrance, when θ approaches 0° or 180°. Essentially the same results are obtained for the range $180° < \theta < 360°$.

The calculations further demonstrate that θ mainly influences the spin density at ring A with $A_{iso}(2^1)$ being smallest for a perpendicular orientation of the acetyl group. The effect on the hfc of ring C is weaker and opposite, that is, $A_{iso}(12^1)$ is largest at $\theta = 90°$. This causes the ratio R to vary strongly with θ. Furthermore, it is found that $A_{iso}(2^1) < A_{iso}(12^1)$ in the vicinity of the energy minima. This is the rationale for assigning the smaller hfc in each spectrum to the methyl group at position 2 and the larger one to position 12. In addition, the results show that two distinct conformations of BPh $a^{\bullet-}$ may exist that differ in the orientation of the 3-acetyl group. It is interesting to note that the calculated hfc's ($A_{iso}(2^1) = 8.2$ MHz, $A_{iso}(12^1) = 9.9$ MHz) and the ratio $R = 1.20$ for the absolute minimum of the total energy ($\theta \approx 135°$) are in good agreement with the experimental values for the $I_2^{\bullet-}$ state of the wild type (Table 1). The ratio $R = 1.27$ measured for the $I_1^{\bullet-}$ state corresponds to $\theta \approx 45°$, which is the second energy minimum of BPh $a^{\bullet-}$. However, the predicted methyl hfc's for this angle are somewhat larger than the experimental values. The ratio R predicted for the absolute minimum also fits well to the experimental value of BPh $a^{\bullet-}$ (and BChl $a^{\bullet-}$) in frozen organic solvents (Table 1), but again the methyl hfc's are generally different. Such differences between predicted and measured hfc's are not surprising in view of the approximations made in the calculations, including the neglect of ring puckering and the protein environment. Nevertheless, the agreement is good enough to allow for a qualitative interpretation: The reorientation of the acetyl group is the main reason for the spectral differences between the two states $I_1^{\bullet-}$ and $I_2^{\bullet-}$.

Another important factor that influences the electronic structure of BPh $a^{\bullet-}$ is hydrogen bonding to the 13^1-keto group. To assess the effect on the methyl hfc's, calculations were performed, in which a water molecule was placed near the keto group and $\theta = 135°$ was kept constant (W. Lubitz, unpublished results). The hydrogen bond causes a slight increase of $A_{iso}(12^1)$ and a negligible decrease of $A_{iso}(2^1)$. The changes of hfc's increase with decreasing hydrogen bonding distance, but never exceed ~5%.

Effects of Hydrogen Bonds on Φ_A. The methyl hfc's of both $I^{\bullet-}$ states in the mutant EL(L104) differ significantly from that of the wild type. This means that the changes of the LUMO of Φ_A upon removal of the hydrogen bond between Glu L104 and the 13^1-keto group are much larger than expected from calculations of BPh $a^{\bullet-}$, in which a water molecule was placed near the keto group (vide supra). In addition, the changes are qualitatively different: $A_{iso}(2^1)$ is significantly decreased by ~20% with respect to the wild type in the case of $I_2^{\bullet-}$, but increased by 7% in the case of $I_1^{\bullet-}$ (Table 1). $A_{iso}(12^1)$ is increased in the states $I_1^{\bullet-}$ and $I_2^{\bullet-}$ by 14% and 4%, respectively. Such effects cannot simply be explained by the electrostatic influence of the bridging proton on the keto oxygen. It is of particular interest that in EL(L104) $A_{iso}(2^1)$ is *decreased* upon relaxation from $I_1^{\bullet-}$ to $I_2^{\bullet-}$ by about 1 MHz, while the reverse is observed in the wild type. This indicates a possible influence of the mutation on the structural relaxation behavior of $\Phi_A^{\bullet-}$, which on the basis of the above considerations could be interpreted as a change of the torsional potential of the 3-acetyl group. In this respect it is interesting to note that there are indications from recent resonance Raman studies of Φ_A in native and mutant RCs of *R. capsulatus* (*46*) that the torsional potential defining θ is modulated by the removal of the hydrogen bond to the 13^1-keto group. These studies also provide evidence for multiple torsional isomers of the 3-acetyl group independent of the presence of the hydrogen bond from Glu L104. Principally, this is in accordance with our finding and interpretation of the two $I^{\bullet-}$ states in the mutant EL(L104). It is therefore reasonable to assume that the mutation near the 13^1-keto group can affect the orientation of the 3-acetyl group and that this intramolecular long-range effect contributes to the observed differences of the relaxation from $I_1^{\bullet-}$ to $I_2^{\bullet-}$ compared with the wild type. Consequently, the calculation described above is not able to reproduce this effect, since the nuclear geometry of BPh *a*, including θ, is kept fixed.

Removal of the putative hydrogen bond between Trp L100 and the 13^2-methyl ester affects the influence of the relaxation from $I_1^{\bullet-}$ to $I_2^{\bullet-}$ on the methyl proton hfc's. In particular, the increase of $A_{iso}(12^1)$ by 11% is larger than that of $A_{iso}(2^1)$ (9%) as compared to 7% and 17%, respectively, in the wild

type. The ratio *R* remains the same within the experimental error (~2%) in contrast to the wild type, where *R* is decreased by 9%. This possibly also indicates that the torsional potential of the 3-acetyl group is changed by the mutation. On the other hand it must be considered that other nuclear coordinates besides θ might be affected by the mutation that could be involved in the relaxation from $I_1^{\bullet-}$ to $I_2^{\bullet-}$, for example, changes of the geometry of rings D and/or E. In contrast to the mutant EL(L104), where both $I^{\bullet-}$ states are strongly affected, the significance of the effects of WF(L100) on the $I_1^{\bullet-}$ state is not clear. The close resemblance of the hfc's of signals 1−4 of WF(L100) to those of the wild type (Table 1) suggests that this mutation has almost no effect on the $I_1^{\bullet-}$ state. The spectra could be explained by the absence of a hydrogen bond between Trp L100 and the 13^2-ester in the $I_1^{\bullet-}$ state and its formation upon relaxation to $I_2^{\bullet-}$ in the wild type. Breton et al. (*9*) proposed on the basis of FTIR data that a conformational substate of Φ_A might exist with the 13^2-ester free from interaction with Trp L100. It is therefore possible that the formation of a hydrogen bond involving this residue or the increase in strength of such a bond contributes to the structural relaxation of the reduced intermediate electron acceptor in the wild type.

Comparison with Earlier Data. Indications for different conformations of the reduced intermediate electron acceptor in bacterial RCs are known from the work of Tiede et al. (*47*). These authors found evidence from optical difference spectroscopy for a low- and a high-temperature form of the freeze-trapped state $I^{\bullet-}Q_A^{\bullet-}$ in RCs from *Rhodopseudomonas viridis*. They proposed that the observed changes arise from a structural relaxation involving the accessory BChl (B_A). Although such a relaxation might play a role, our data suggest that acetyl rotation of Φ_A could also be important in this process.

Functional Implications. In this paper we have shown that two states, $I_1^{\bullet-}$ and $I_2^{\bullet-}$, of the intermediate BPh acceptor can be trapped in RCs of *R. sphaeroides*. It is interesting to speculate whether two (or even more) distinct conformations of the transient state $P^{\bullet+}\Phi_A^{\bullet-}$ exist that relax during the ET process and contribute to a stabilization of the charge separation. Implications for such a mechanism ("conformational cooling") already exist in the literature and are based on the observed complex kinetics of absorbance difference spectra and delayed fluorescence (*48*−*50*). On the basis of our results it is likely that in the ET process not only alterations of the protein surrounding but also particular structural changes of the chromophores occur. The BPh *a* (Φ_A) is located in a fairly hydrophobic environment in the RC (*1*, *2*). This prevents a large external reorganization energy λ_e upon formation of the $P^{\bullet+}\Phi_A^{\bullet-}$ state. The reduced BPh can, however, undergo an (internal) structural relaxation. On the basis of our data this could involve a rotation of the acetyl group. Inspection of the X-ray crystallographic structure (*2*) shows that this group is essentially free to rotate.

The acetyl "conformational switch" is probably activated by the positive charge on the primary donor, $P^{\bullet+}$. Furthermore, it can be speculated on the basis of our data and that of Bocian and co-workers (*46*) whether the crucial role of the hydogen bond to the 13^1-keto group, which is only found in the A-branch, is to fine-tune the torsional potential of the 3-acetyl group, thereby influencing the relaxation and free-energy changes of $P^{\bullet+}\Phi_A^{\bullet-}$. Additional major contributions to a charge stabilization are expected from an increase of the hydrogen bond strengths to $\Phi_A^{\bullet-}$ compared with neutral Φ_A involving residues Glu L104 and Trp L100. This has been discussed earlier for L104 by Bylina et al. (*5*) for *R. capsulatus* and has also been found for the mutation in *R. sphaeroides* (Allen et al., unpublished results). The trapped states occurring in our experiments on $I^{\bullet-}$ cannot represent all the possible processes that could take place during the charge separation, but they allow us to identify some of the structural changes that are probably important in RC function on a molecular level.

CONCLUSIONS AND OUTLOOK

Our results corroborate the common view that in RCs of *R. sphaeroides* the BPh in the A-branch is selectively reduced in freeze-trapping experiments. The radical anion can be obtained in two distinct conformations, called $I_1^{\bullet-}$ and $I_2^{\bullet-}$, which presumably differ in the orientation of the 3-acetyl group. Each of the two conformations probably exists in different subconformers, for example, conformations with a twist of the saturated rings or torsional isomers of other substituents such as the 13^2-methyl ester. The occurrence of these subconformers appears to be influenced by mutations and/or quinone extraction. The *irreversible* transition from $I_1^{\bullet-}$ to $I_2^{\bullet-}$ is frozen out at temperatures below 160 K. On the basis of the ENDOR spectra we conclude that the hydrogen bond between Glu L104 and the 13^1-keto group of Φ_A is present in both conformations. The hydrogen bond between Trp L100 and the 13^2-methyl ester is possibly weakened or absent in the $I_1^{\bullet-}$ state. It is proposed that the conformational states, involving acetyl rotation, hydrogen bond formation, etc., play a role in the stabilization of the charge-separated states in the RC. To test the hypothesis that the reorientation of the 3-acetyl group is responsible for the occurrence of two freeze-trapped $I^{\bullet-}$ states, we are presently investigating mutants with changes at position M210, which could influence the torsional motion of the acetyl group. These studies will eventually contribute to a more detailed understanding of the initial charge separation process in photosynthesis.

ACKNOWLEDGMENT

We are indebted to Dr. E. Schlodder (TU Berlin) for determining the quinone content of RC samples and to Dr. M. Plato (FU Berlin) for his help with the INDO calculations and many helpful discussions. Furthermore, we thank Dr. H. Axelrod (UC San Diego) for providing a protocol for the preparation of cyt c_2 and Prof. Dr. D. Bocian (UC Riverside) for sending us manuscripts prior to publication. ENDOR/Special TRIPLE accessories were developed by Drs. F. Lendzian and R. Bittl (both TU Berlin). The software used to simulate hf powder patterns was written by Dr. H. Käss at the TU Berlin. We also thank I. Geisenheimer and R. Kunert (both TU Berlin) for technical assistance as well as Dr. J. Rautter (TU Berlin) for valuable help in the initial phase of the project. Stimulating discussions with Prof. Dr. M. Y. Okamura (UC San Diego) and Prof. Dr. R. J. Cogdell (University of Glasgow) are gratefully acknowledged.

REFERENCES

1. Feher, G., Allen, J. P., Okamura, M. Y., and Rees, D. C. (1989) *Nature 339*, 111−116.

2. Ermler, U., Fritzsch, G., Buchanan, S., and Michel, H. (1994) *Structure 2*, 925−936.
3. Woodbury, N. W., and Allen, J. P. (1995) in *Anoxygenic Photosynthetic Bacteria* (Blankenship, R. E., Madigan, M. T., and Bauer, C. E., Eds.) pp 527−557, Kluwer Academic Publishers, Dordrecht, The Netherlands.
4. Heller, B. A., Holten, D., and Kirmaier, C. (1995) *Science 269*, 940−945.
5. Bylina, E. J., Kirmaier, C., McDowell, L., Holten, D., and Youvan, D. C. (1988) *Nature 336*, 182−184.
6. Kirmaier, C., Laporte, L., Schenck, C. C., and Holten, D. (1995) *J. Phys. Chem. 99*, 8903−8909.
7. Kirmaier, C., Laporte, L., Schenck, C. C., and Holten, D. (1995) *J. Phys. Chem. 99*, 8910−8917.
8. Lubitz, W., Müh, F., Rautter, J., Lendzian, F., Allen, J. P., and Williams, J. C. (1995) in *Photosynthesis: from Light to Biosphere, Vol. I* (Mathis, P., Ed.) pp 413−418, Kluwer Academic Publishers, Dordrecht, The Netherlands.
9. Breton, J, Nabedryk, E., Allen, J. P., and Williams, J. C. (1997) *Biochemistry 36*, 4515−4525.
10. Kirmaier, C., Holten, D., and Parson, W. W. (1985) *Biochim. Biophys. Acta 810*, 49−61.
11. Michel-Beyerle, M. E., Plato, M., Deisenhofer, J., Michel, H., Bixon, M., and Jortner, J. (1988) *Biochim. Biophys. Acta 932*, 52−70.
12. Okamura, M. Y., Isaacson, R. A., and Feher, G. (1979) *Biochim. Biophys. Acta 546*, 394−417.
13. Shuvalov, V. A., and Klimov, V. V. (1976) *Biochim. Biophys. Acta 440*, 587−599.
14. Tiede, D. M., Prince, R. C., and Dutton, P. L. (1976) *Biochim. Biophys. Acta 449*, 447−467.
15. van Grondelle, R., Romijn, J. C., and Holmes, N. G. (1976) *FEBS Lett. 72*, 187−192.
16. Kurreck, H., Kirste, B., and Lubitz, W. (1988) *Electron Nuclear Double Resonance Spectroscopy of Radicals in Solution, Application to Organic and Biological Chemistry* (Marchand, A. P., Ed.) VCH Publishers, Weinheim, Germany.
17. Möbius, K., Lubitz, W., and Plato, M. (1989) in *Advanced EPR* (Hoff, A. J., Ed.) pp 441−499, Elsevier, Amsterdam, The Netherlands.
18. Lubitz, W. (1991) in *Chlorophylls* (Scheer, H., Ed.) pp 903−944, CRC Press, Boca Raton, FL.
19. Lubitz, W., and Lendzian, F. (1996) in *Biophysical Techniques in Photosynthesis* (Amesz, J., and Hoff, A. J., Eds.) pp 255−275, Kluwer Academic Publishers, Dordrecht, The Netherlands.
20. Feher, G., Isaacson, R. A., and Okamura, M. Y. (1977) *Biophys. J. (Abstr.) 17*, 149.
21. Fajer, J., Forman, A., Davis, M. S., Spaulding, L. D., Brune, D. C., and Felton, R. H. (1977) *J. Am. Chem. Soc. 99*, 4134−4140.
22. Feher, G., Isaacson, R. A., Okamura, M. Y., and Lubitz, W. (1987) *Biophys. J. (Abstr.) 51*, 377a.
23. Lubitz, W., Plato, M., Feher, G., Isaacson, R. A., and Okamura, M. Y. (1988) *Biophys. J. (Abstr.) 53*, 67a.
24. Feher, G., Isaacson, R. A., Okamura, M. Y., and Lubitz, W. (1988) in *The Photosynthetic Bacterial Reaction Center* (Breton, J., and Vermeglio, A., Eds.) pp 229−235, Plenum Press, New York.
25. Williams, J. C., Alden, R. G., Murchison, H. A., Peloquin, J. M., Woodbury, N. W., and Allen, J. P. (1992) *Biochemistry 31*, 11029−11037.
26. Feher, G., and Okamura, M. Y. (1978) in *The Photosynthetic Bacteria* (Clayton, R. K., and Sistrom, W. R., Eds.) pp 349−386, Plenum Press, New York.
27. Buchanan, S. K., Fritzsch, G., Ermler, U., and Michel, H. (1993) *J. Mol. Biol. 230*, 1311−1314.
28. Straley, S. C., Parson, W. W., Mauzerall, D. C., and Clayton, R. K. (1973) *Biochim. Biophys. Acta 305*, 597−609.
29. Okamura, M. Y., Debus, R. J., Kleinfeld, D., and Feher, G. (1982) in *Function of Quinones in Energy Conserving Systems* (Trumpower, B. L., Ed.) pp 299−317, Academic Press, New York.
30. Axelrod, H. L., Feher, G., Allen, J. P., Chirino, A., Day, M., Hsu, B. T., and Rees, D. C. (1994) *Acta Crystallogr., Sect. D 50*, 596−602.
31. Rautter, J., Lendzian, F., Lubitz, W., Wang, S., and Allen, J. P. (1994) *Biochemistry 33*, 12077−12084.
32. Zweygart, W., Thanner, R., and Lubitz, W. (1994) *J. Magn. Reson., Ser. A 109*, 172−176.
33. Käss, H., Rautter, J., Zweygart, W., Struck, A., Scheer, H., and Lubitz, W. (1994) *J. Phys. Chem. 98*, 354−363.
34. Debus, R. J., Feher, G., and Okamura, M. Y. (1985) *Biochemistry 24*, 2488−2500.
35. Müh, F., Rautter, J., and Lubitz, W. (1996) *Ber. Bunsen-Ges. Phys. Chem. 100*, 1974−1977.
36. Müh, F., Rautter, J., and Lubitz, W. (1997) *Biochemistry 36*, 4155−4162.
37. Katz, J. J., Dougherty, R. C., Crespi, H. L., and Strain, H. H. (1966) *J. Am. Chem. Soc. 88*, 2856−2857.
38. Bönigk, B. (1994) Doctoral Thesis, Technische Universität Berlin, Germany.
39. Hyde, J. S., Rist, G. H., and Eriksson, L. E. G. (1968) *J. Phys. Chem. 72*, 4269−4275.
40. Bersohn, R. (1956) *J. Chem. Phys. 24*, 1066−1070.
41. Heller, C., and McConnell, H. M. (1960) *J. Chem. Phys. 32*, 1535−1539.
42. Atherton, N. M. (1993) *Principles of Electron Spin Resonance*, Ellis Horwood PTR Prentice Hall, Chichester, New York.
43. Dinse, K., Biehl, R., and Möbius, K. (1974) *J. Chem. Phys. 61*, 4335−4341.
44. Plato, M., Möbius, K., and Lubitz, W. (1991) in *Chlorophylls* (Scheer, H., Ed.) pp 1015−1046, CRC Press, Boca Raton, FL.
45. Hanson, L. K., Thompson, M. A., Zerner, M. C., and Fajer, J. (1988) in *The Photosynthetic Bacterial Reaction Center* (Breton, J., and Vermeglio, A., Eds.) pp 355−367, Plenum Press, New York.
46. Cua, A., Kirmaier, C., Holten, D., and Bocian, D. F. (1998) *Biochemistry 37*, 6394−6401.
47. Tiede, D. M., Kellogg, E., and Breton, J. (1987) *Biochim. Biophys. Acta 892*, 294−302.
48. Peloquin, J. M., Williams, J. C., Lin, X., Alden, R. G., Taguchi, A. K. W., Allen, J. P., and Woodbury, N. W. (1994) *Biochemistry 33*, 8089−8100.
49. Holzwarth, A. R., and Müller, M. G. (1996) *Biochemistry 35*, 11820−11831.
50. van Stokkum, I. H. M., Beekman, L. M. P., Jones, M. R., van Brederode, M. E., and van Grondelle, R. (1997) *Biochemistry 36*, 11360−11368.

BI980799F